

Turn-key module for neutron scattering with sub-micro-eV resolution

R. Georgii,^{1,2, a)} G. Brandl,^{2,1} N. Arend,^{3,2} W. Häußler,^{1,2} A. Tischendorf,² C. Pfeleiderer,² P. Böni,² and J. Lal⁴

¹⁾ *Forschungsneutronenquelle Heinz-Maier Leibnitz, Technische Universität München, 85748 Garching, Germany*

²⁾ *Physik-Department E21, Technische Universität München, 85748 Garching, Germany*

³⁾ *Forschungszentrum Jülich GmbH, JCNS-1 & ICS-1, Oak Ridge National Laboratory, Oak Ridge, TN 37831, USA*

⁴⁾ *Materials Science Division, Argonne National Lab, Argonne IL-60439, USA*

(Dated: 12 January 2013)

We report the development of a compact turn-key module that boosts the resolution in quasi-elastic neutron scattering by several orders of magnitude down to the low sub- μeV range. It is based on a pair of neutron resonance spin flippers that generate a well defined temporal intensity modulation, also known as MIEZE (Modulation of Intensity by Zero Effort). The module may be used under versatile conditions, in particular in applied magnetic fields and for depolarising and incoherently scattering samples. We demonstrate the power of MIEZE in studies of the helimagnetic order in MnSi under applied magnetic fields.

©(2011) American Institute of Physics. This article may be downloaded for personal use only. Any other use requires prior permission of the author and the American Institute of Physics.

The following article appeared in Applied Physics Letters and may be found at URL: <http://link.aip.org/link/?apl/98/073505>

Neutron scattering is an extremely powerful technique for studies of the dynamical properties of condensed matter systems. Prominent examples of great current interest concern the spin dynamics in transition metal and rare earth compounds and diffusive processes in soft matter systems such as proteins, liquid crystals and emulsions. A precondition to unravel some of the most important scientific challenges is the need for high energy and momentum resolution.

Conventional neutron scattering techniques such as triple-axis and time-of-flight spectroscopy provide momentum resolved energy resolutions of the order of $\simeq 10 \mu\text{eV}$. Backscattering reaches the sub- μeV regime, however sacrificing momentum resolution. This is contrasted by neutron spin-echo (NSE) methods^{1,2}, which offer high energy and momentum resolutions in the low sub- μeV range – several orders of magnitude below the typical resolutions of conventional techniques. However, because NSE scattering uses polarised neutrons it is inherently sensitive to the depolarisation of the neutron beam. Therefore, it is technically very demanding to perform NSE measurements under applied magnetic fields or in depolarising samples^{3,4} such as superconductors, ferromagnets⁵ or protonated soft matter systems.

In this Letter we report the development of a turn-key module, the MIEZE box shown in Fig. 1. In combination with a polariser, a polarising analyser and a fast detector this box allows to improve the energy resolution in all types of neutron scattering instruments capable of studying quasi-elastic scattering, notably diffractometers, small-angle neutron scattering cameras and reflectometers (especially instruments for small q and cold

neutrons), down to the sub- μeV range. The module is based on the so-called MIEZE-I technique (Modulation of Intensity by Zero Effort, type I)^{6–11}, where the modulation of the beam is performed upstream of the sample. Therefore, in contrast to NSE, the MIEZE module we describe may even be used under depolarising conditions in or around the sample. This routinely allows neutron scattering studies with the highest possible energy resolution in a wide range of materials.

Qualitatively, the MIEZE-I technique is based on a harmonic intensity modulation of the neutron beam, where the contrast C is given by the ratio of the amplitude A to the average signal B as shown in Fig. 2a. Us-

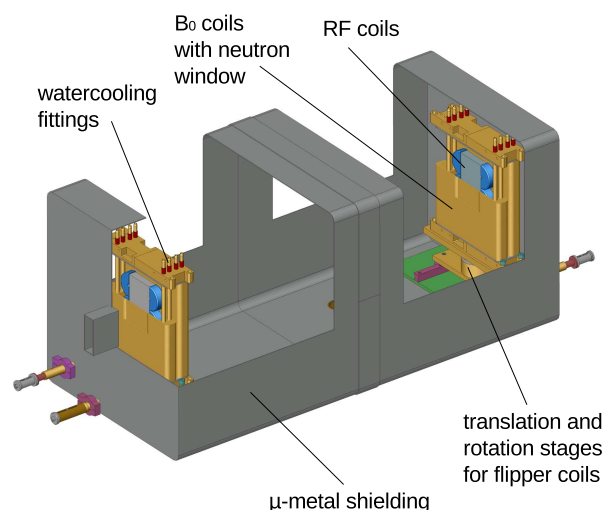


FIG. 1. The “MIEZE box” as used for the MIEZE setup at MIRA.

^{a)} Electronic mail: Robert.Georgii@frm2.tum.de

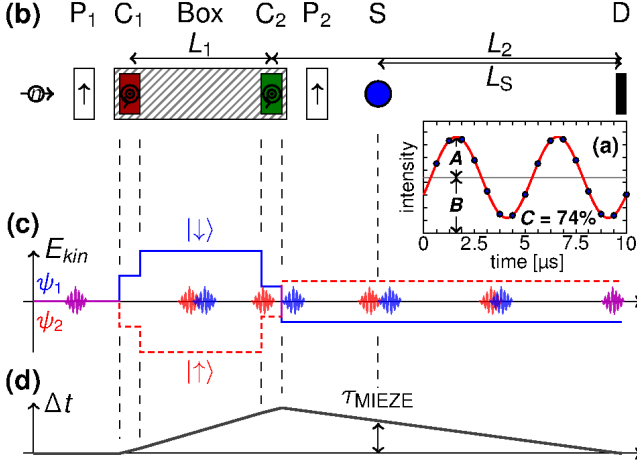


FIG. 2. (a) A typical MIEZE signal at the detector position (see text for details). (b) Schematic of a complete MIEZE setup, showing the polariser (P_1), the zero field of the MIEZE box (hatched) with two π -flipper coils (C_1 , C_2), the analyser (P_2), the sample (S) and the detector (D). (c) Kinetic energy splitting for the spin-down (ψ_1) and spin-up (ψ_2) states of the neutrons along the flight path due to the π -flipper coils. (d) Temporal delay Δt of the spin states along the flight path. The splitting reaches its maximum after the second flipper coil and vanishes at the detector position.

ing a phase-locked pair of two resonance spin flippers^{9,13}, which operate at slightly different frequencies, ν_1 and ν_2 , induces a slow rotation of the polarisation direction of the neutrons, which is subsequently converted into an intensity beating by means of a polarising analyser.

While former experiments with the MIEZE-I technique have been successful, we managed to implement MIEZE-I as a routine technique through a redesign of the neutron resonance spin flippers. Instead of wire-wound B_0 coils we use electro-erosion machined coil windings where a better definition of the magnetic field boundaries is obtained. They consist of a specially selected Al alloy with much less small angle scattering and a higher transmission¹³. Together with a more reproducible mounting of the RF coils this results in stable π -flips over a wide range of RF frequencies with low small angle scattering background.

A description of the MIEZE-I principle pointing out its vicinity to TOF methods is illustrated in Fig. 2; for a proper quantum mechanical description we refer to the literature (cf Ref. ¹⁴). When a neutron arrives at the first spin flipper with its polarisation perpendicular to the static field in the flipper, the correlation volumes (or wave-packages) corresponding to the spin-up and spin-down spin states are prepared (cf Fig. 2(c)). While the kinetic energy of the spin-down state increases, the kinetic energy of the spin-up state decreases. Therefore, the correlation volumes for the spin-down and spin-up states arrive at different times at the second resonance spin flipper placed at a distance L_1 behind the first spin flipper. This second spin flipper inverts the energy split-

ting of the spin states, reducing the kinetic energy of the spin-down state and increasing the kinetic energy of the spin-up state. Therefore the correlation volumes, overlap again at a distance L_2 behind the second spin flipper, given by $L_2 = L_1 (\nu_2/\nu_1 - 1)^{-1}$ where $\nu_2 > \nu_1$.

An analyser at an arbitrary position between the second spin flipper and the detector (the latter is located where the correlation volumes meet) projects out the intensity of the interference pattern of the spin-up and spin-down states. As the correlation volumes of the spin-up and spin-down states have different energies, the interference pattern exhibits the intensity modulation of contrast C referred to above.

To explain how this intensity modulation may be exploited in experimental studies using two single neutron resonance spin flippers, we show in Fig. 2(d) the delay between the two correlation volumes, Δt . The correlation volumes probe the sample at different times with the delay given by¹⁵ $\tau_{\text{MIEZE}} = 2 \cdot \hbar(2\pi\Delta\nu)L_S/(mv^3)$, where $2\Delta\nu = 2(\nu_2 - \nu_1)$ is the frequency of the resulting MIEZE signal, L_S is the distance between sample and detector, and m and v are the mass and average velocity of the neutrons. By overlapping these volumes at the detector, one obtains a signal contrast C which is directly proportional to the intermediate scattering function $S(q, \tau_{\text{MIEZE}})$, i.e., the information on the dynamics on this time scale. Further, for quasi-elastic scattering with an assumed Lorentzian line shape with half-width Γ , the normalised intermediate scattering function is given by⁹ $S(q, \tau)/S(q, 0) = \exp(-\Gamma(q)\tau)$, where $S(q, 0)$ corresponds to the intermediate scattering function of a purely elastically scattering sample.

The MIEZE-I technique is similar to conventional neutron resonance spin echo (NRSE) methods, where the two spin flippers before the sample correspond to the first arm of an NRSE instrument. Moreover, the MIEZE time τ_{MIEZE} is equivalent to the spin echo time in NSE and NRSE instruments⁹. However, there is a distinct difference between MIEZE-I and NSE/NRSE. Placing the polarising analyser behind the second spin flipper and before the sample, the MIEZE-I technique becomes insensitive to effects of the sample or sample environment on the polarisation of the neutron beam, i.e. for example depolarisation or applied magnetic fields. This is demonstrated in Fig. 3, where the contrast of the direct beam is plotted versus a magnetic field up to 0.2 T and no effect on the signal contrast can be observed.

The MIEZE experiments were carried out at the diffractometer MIRA at FRM II using neutrons with a wavelength $\lambda = 10.4 \text{ \AA} \pm 5\%$, i.e., a mean velocity $v = 380 \text{ m/s}$. The first and second spin flipper being 0.9 m apart were operating at frequencies in the range $46 \text{ kHz} < \nu_1 < 200 \text{ kHz}$ and $69 \text{ kHz} < \nu_2 < 300 \text{ kHz}$, respectively, providing a beating frequency in the range $46 \text{ kHz} < 2\Delta\nu < 200 \text{ kHz}$. The distance between the sample and detector was 860 mm. Taken together MIEZE times could be accessed in a range $280 \text{ ps} < \tau_{\text{MIEZE}} < 1230 \text{ ps}$. A 0.3 mm thick ^6Li doped

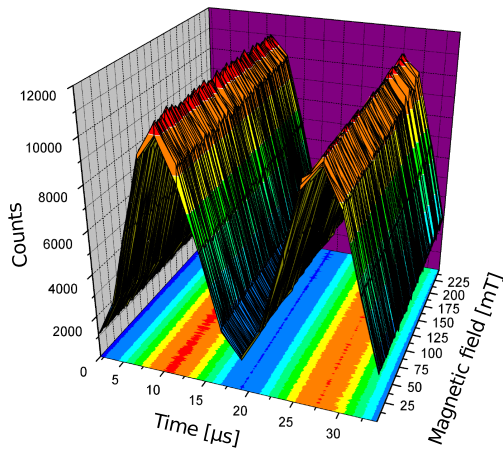


FIG. 3. The MIEZE signal for the direct beam and a magnetic field produced with an electromagnet¹³. Note that the contrast does not depend on the field strength.

glass scintillator with a photomultiplier was used as a fast detector.

We note that the temporal and thus spatial separation of the spin-up and spin-down states makes MIEZE-I sensitive to path length differences between the first RF-flipper and the detector, e.g. due to the large divergence of the beam, the finite size of the sample or the finite thickness of the neutron detector. However, for the wavelength of 10.4 Å, frequencies in the range 46 kHz to 200 kHz for the MIEZE signal, typical sample sizes of 10 mm, and scattering angles of the order of a few degrees we measured with a standard sample used for resolution measurements a contrast reduction of less than 10% up to $q = 0.05 \text{ Å}^{-1}$ being in agreement with the results of calculations of the path length and precession phase differences.

To demonstrate the power of MIEZE-I in studies of field-induced forms of magnetic order normally not accessible to NSE/NRSE, we have investigated the cubic B20 compound MnSi¹⁶. MnSi orders helimagnetically below a transition temperature, in our case at $T_c = 29.0 \text{ K}$. The large pitch of the helix $\Lambda \approx 180 \text{ Å}$ implies that the associated magnetic Bragg peak at $q = 0.035 \text{ Å}^{-1}$ can be accessed in a forward scattering configuration. Just below T_c at $0.15 \text{ T} < B < 0.2 \text{ T}$, the A-phase is observed. Here a special form of magnetic order, a skyrmion lattice, is observed¹⁷.

Shown in Fig. 4 (a) are typical data in the helimagnetic state ($B = 0$) of the normalised intermediate scattering function $S(q, \tau)/S(q, 0)$ for various temperatures. Data were normalised with respect to resolution measurements in the helical ordered sample at low temperatures, where the magnetic structure is supposed to be static. The solid lines are the result of fits to exponential functions. The presence of a second process on a shorter timescale as indicated by the fact that the fits are not converging to 1 for $\tau \rightarrow 0$ around T_c is still under discussion and

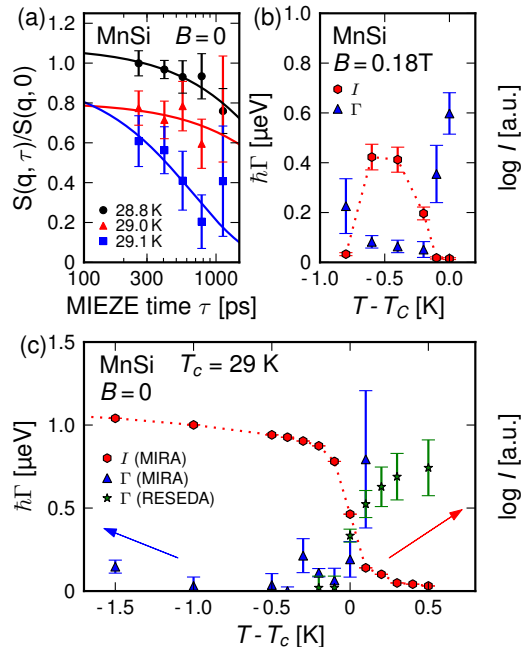


FIG. 4. (a) Typical normalised intermediate scattering functions $S(q, \tau)$ in the helimagnetic state of MnSi at selected temperatures. (b) Line width Γ in the A-phase of MnSi at $B = 0.18 \text{ T}$. The total scattering intensity is shown as solid hexagons, MIEZE data as solid triangles. The data are normalised to the line width of the helical phase at $T = 3 \text{ K}$. (c) Line width Γ of the magnetic order in MnSi at $B = 0$. The data are normalised to the line width at $T = 3 \text{ K}$. NRSE data from the instrument RESEDA are shown as stars.

will be published elsewhere. The resulting line widths (solid triangles) as a function of temperature are shown in Fig. 4 (c) (solid hexagones show the elastic magnetic intensity). While the magnetic order is resolution limited below T_c , there is broadening above T_c . For comparison, NRSE data from the same system are shown as stars.

The measured Γ in the A-Phase of MnSi at $B = 0.18 \text{ T}$ (shown in Fig. 4 (b)) is similar to the one in the helical phase. This demonstrates that even under applied magnetic fields the MIEZE-I technique may be readily used.

We have recently used our MIEZE box at the beam line CG-1D at HFIR at Oak Ridge National Laboratory¹². Here and on MIRA to set up and adjust the MIEZE box requires less than a few hours making it indeed a turn-key measurement option.

In conclusion we have developed a compact turn-key MIEZE module, that allows to improve the energy resolution of various neutron scattering instruments used for quasi-elastic scattering into the sub- μeV range for typical sample sizes of 1 cm in diameter and q values up to 0.05 Å^{-1} . We have demonstrated the power of this technique by small angle scattering studies of the magnetic order of MnSi in applied magnetic fields. One particular strength of the MIEZE-I technique is its insensitivity to depolaris-

ing conditions at the sample position, which is not easily achievable using standard spin echo techniques. This illustrates the wide range of scientific challenges that may now be addressed with sub- μeV resolution.

We gratefully acknowledge support by R. Schwikowski, A. Mantwill, M. Wipp and the team of FRM II. Many thanks to R. Gähler, L. Robertson, I. Anderson and W. Petry for helpful discussions and support. Financial support through the German Science Foundation (DFG), the Oak Ridge National Laboratory and the European Commission under the 7th Framework Program, Contract no. CP-CSA INFRA-2008-1.1.1 Number 226507-NMI3 is acknowledged.

¹F. Mezei, Z. Phys. A, **255**, 146 (1972).

²R. Golub and R. Gähler, Phys. Lett. A, **123**, 43 (1987).

³C. Pappas, E. Lelievre-Berna, P. Bentley, E. Bourgeat-Lami, E. Moskvina, M. Thomas, S. Grigoriev, and V. Dyadkin, NIM A, **592**, 420 (2008).

⁴C. Pappas, E. Lelievre-Berna, P. Falus, P. M. Bentley, E. Moskvina, S. Grigoriev, P. Fouquet, and B. Farago, Phys. Rev. Lett., **102**, 197202 (2009).

⁵B. Farago and F. Mezei, Physica B, **136**, 100 (1986).

⁶R. Gähler, R. Golub, and T. Keller, Physica B, **180-181**, 899 (1992).

⁷M. Köppe, P. Hank, J. Wuttke, W. Petry, R. Gähler, and R. Kahn, J. Neutron Res., **4**, 261 (1996).

⁸W. Besenböck, R. Gähler, P. Hank, R. Kahn, M. Köppe, C. H. D. Novion, W. Petry, and J. Wuttke, J. Neutron Res., **7**, 65 (1998).

⁹T. Keller, R. Golub, and R. Gähler, in *Scattering and Inverse Scattering in Pure and Applied Science* (Academic Press, London, 2002) pp. 1264–1286.

¹⁰M. Bleuel, M. Bröll, E. Lang, K. Littrell, R. Gähler, and J. Lal, Physica B, **371**, 297 (2006).

¹¹Y. Kawabata, M. Hino, M. Kitaguchi, H. Hayashida, S. Tasaki, T. Ebisawa, D. Yamazaki, R. Maruyama, H. Seto, M. Nagao, and T. Kanaya, Physica B, **385-386**, 1122 (2006).

¹²G. Brandl, M. Bleuel, L. Robertson, L. Crow, J. Lal, and R. Georgii, Unpublished.

¹³N. Arend, Ph.D. thesis, Technical University of Munich (2007).

¹⁴N. Arend, R. Gähler, T. Keller, R. Georgii, T. Hils, and P. Böni, Phys. Lett. A, **327**, 21 (2004).

¹⁵The pre-factor 2 is inherent to the NRSE/MIEZE technique when using the resonance flippers in the non-bootstrap mode.

¹⁶Y. Ishikawa, K. Tajima, D. Bloch, and M. Roth, Solid State Commun., **19**, 525 (1976).

¹⁷S. Mühlbauer, B. Binz, F. Jonietz, C. Pfleiderer, A. Rosch, A. Neubauer, R. Georgii, and P. Böni, Science, **323**, 915 (2009).